EFDA–JET–PR(10)36

M. Valisa, L. Carraro, I. Predebon, M.E. Puiatti, C. Angioni, I. Coffey, C. Giroud, L. Lauro Taroni, B. Alper, M. Baruzzo, P. Belo daSilva, P. Buratti, L. Garzotti, D. Van Eester, E. Lerche, P. Mantica, V. Naulin, T. Tala, M. Tsalas and JET EFDA contributors

Metal Impurity Transport Control in JET H-mode Plasmas with Central Ion Cyclotron Radio Frequency Power Injection

Metal Impurity Transport Control in JET H-mode Plasmas with Central Ion Cyclotron Radio Frequency Power Injection

M. Valisa[1], L. Carraro[1], I. Predebon[1], M.E. Puiatti[1], C. Angioni[2], I. Coffey[3], C. Giroud[4], L. Lauro Taroni[1], B. Alper[4], M. Baruzzo[1], P. Belo daSilva[5], P. Buratti[6], L. Garzotti[4], D. Van Eester[7], E. Lerche[7], P. Mantica[8], V. Naulin[9], T. Tala[10], M. Tsalas[11] and JET EFDA contributors*

JET-EFDA, Culham Science Centre, OX14 3DB, Abingdon, UK

[1]Consorzio RFX – Associazione EURATOM-ENEA sulla Fusione, Padova, Italy
[2]Max Planck Institut fur Plasmaphysik, EURATOM-IPP Association, D-85748 Garching, Germany
[3]Department of Physics, Queen's University, Belfast, United Kingdom
[4]EURATOM-CCFE Fusion Association, Culham Science Centre, OX14 3DB, Abingdon, OXON, UK
[5]EURATOM/IST 5Fusion Association, Instituto de Plasmas e Fusão Nuclear, Avenue Rovisco Pais 1049-001 Lisbon Portugal
[6]EURATOM-ENEA Association, C.R. Frascati, CP 65, 00044 Frascati, Italy
[7]Association EURATOM-Belgian State, LPP-ERM/KMS, Partner in TEC, B-1000 Brussels, Belgium
[8]Associazione EURATOM-ENEA sulla Fusione, Via Cozzi, Milano, Italy
[9]Association EURATOM - Risoe DTU, Frederiksborgvej 399, 4000 Roskilde, Denmark
[10]Association Euratom-Tekes, VTT, P.O. Box 1000 FI-02044 VTT –Finland
[11]EFDA CSU Culham, Culham Science Centre, Abingdon,OX14 3DB, UK
** See annex of F. Romanelli et al, "Overview of JET Results", (23rd IAEA Fusion Energy Conference, Daejon, Republic of Korea (2010)).*

Preprint of Paper to be submitted for publication in Nuclear Fusion

ABSTRACT

The scan of Ion Cyclotron Resonant Heating power has been used to systematically study the pump out effect of central electron heating on impurities such as Ni and Mo in H mode low collisionality discharges in JET. The transport parameters of Ni and Mo have been measured by introducing a transient perturbation on their densities via the Laser Blow Off technique. Without ICRH, Ni and Mo density profiles are typically peaked. The application of ICRH, induces on Ni and Mo in the plasma center (at normalized poloidal flux $\rho = 0.2$) an outward drift approximately proportional to the amount of injected power. Above a threshold, of about 3MW of ICRH power in the specific case, the radial flow of Ni and Mo changes from inward to outward and the impurity profiles, extrapolated to stationary conditions, become hollow. At mid radius the impurity profiles become flat or only slightly hollow. In the plasma centre the variation of the pinch parameter v/D of Ni is particularly well correlated with the change of the ion temperature gradient, in qualitative agreement with the neoclassical theory. However, the experimental radial velocity is larger than the neoclassical one by up to one order of magnitude. Gyrokinetic simulations of the radial impurity fluxes induced by electrostatic turbulence do not foresee a flow reversal in the analyzed discharges.

1. INTRODUCTION

The relevance of the impurity transport studies in fusion plasmas relies on the fact that in the core of a fusion reactor the fuel dilution, the main ion to electron density ratio, must be as close as possible to 1 to ensure an efficient fusion yield. In ITER, for instance, the effective charge Z_{eff} is specified to be below 1.5, including fusion reaction ashes [18]. ITER will feature tungsten tiles in the divertor and highly radiating elements could be additionally injected to build up a radiation shield at the edge to protect the wall. It is therefore important that the physics underlying the impurity behavior in a reactor relevant plasma is well understood and in particular that an active feedback tool is conceived to control the impurity concentration in any situation.

In a diverted Tokamak plasma the content of impurities in the centre is the result of a complex series of processes that regard their production on the in-vessel components, their transport across the scrape off layer and the steep pressure gradients of the plasma edge, as well as their trip through the main plasma. A comprehensive study of the impurity behavior is beyond the scope of this paper where we focus on the centre and centre and core regions in the attempt of better understanding the processes that may lead to a reliable control of the metal impurity density profiles.

It is a well known fact, documented in various experiments, that additional central heating, especially electron heating , has a flattening effect on the density profiles of impurities in the plasma core and may reverse the impurity radial convection from being typically inward to outward [31, 8, 36, 35, 13, 37, 6, 34]. Similar findings are reported also in non axisymmetric devices [4]. Incidentally, a significant outward convection for Ni has been reported in a Reversed Field Pinch, characterized by strong central ohmic (i.e electron) heating [24]. In recent ASDEX Upgrade campaigns with a full W wall, Electron Cyclotron Radiofrequency Heating (ECRH) was routinely used to avoid W

accumulation in the centre [28,29] and a similar effect, though not as efficient, was reported upon application of ICRH or neutral beam heating [28].

The origin of such an inversion of the impurity radial flow is not well understood. In a previous publication [34] we had shown how in JET the impurity radial flow reversal induced by the application of ICRH in the H or He minority scheme, to heat preferentially electrons, could not be satisfactorily understood in the light of electrostatic turbulence analysis. In the JET conditions explored in [34] in fact, with the normalized logarithmic gradients R/L_{Ti} between 6 and 10, R/L_{Te} between 4 and 10 and R/L_{ne} between 2 and 4, the curvature (compressional) pinch driven by the dominating turbulent modes, the Ion Temperature Gradient (ITG) modes, would result in an inward pinch opposite than in the experiment. At mid radius ($\rho = 0.5$, where r is the normalized poloidal flux coordinate) subdominant Trapped Electron Modes (TEM's) induced by parallel fluctuations were indeed found to contribute to the flow with an outward component, as in the experiment [1], but the dominant ITG modes were pushing impurities inward. The neoclassical contribution was negligible. In ASDEX Upgrade, in a similar context of additional electron heating applied to hinder the impurity build up in the plasma centre with R/L_{Ti} within 4 and 6, R/L_{Te} between 4 and 10 and R/L_{ne} between 2 and 4, Trapped Electron Modes have been found to emerge and produce an outward flow [2], in agreement with the experimental finding.

Besides the AUG case mentioned above there are few other examples in the recent literature in which turbulent theory seems to reproduce the experimental transport of impurities. In Tore Supra ohmic regimes with dominant electron heating, R/L_{Ti} within 4 and 10, R/L_{Te} between 6 and 10, the inward flow of several impurity species is coherent with quasi linear gyrokinetic calculations [14,38]. In JET H-mode discharges where the dependence of impurity transport on Z was investigated, a qualitative analogy between the numerical predictions, especially of its thermodiffusion component, and the experimentally evaluated anomalous component of the flow was found [12]. In DIII-D Very High Confinement discharges with reduced turbulent transport, small density gradients and large ion temperature gradients, medium/low Z impurities were found to be expelled by the strong temperature screening of neoclassical nature, with a strong Z dependence [39]. In general, however, central electron heating induces a turbulent pinch that is larger than the neoclassical convection (2, 37, 34, 12].

Theory has indeed experienced a significant growth of interest for the behavior of impurities in the recent years. The quasi linear theory has identified several terms that contribute to the radial transport [1,9,26]. Perpendicular compressibility induces a curvature pinch velocity typically directed inward, independent of the impurity charge Z, and changes sign with the magnetic shear. Parallel compressibility determines instead a contribution that depends on the phase velocity of the fluctuations (outward for TEM and inward for ITG modes) and is proportional to the ratio of the impurity charge to the mass ratio. The temperature gradient is responsible for a term (thermodiffusion) whose direction depends on the direction of propagation of the dominant turbulence modes (inward for TEM and outward for ITG modes) and is proportional to 1/Z. In general the contribution of

the latter term is however found to be negligible [34, 14]. By means of a three-dimensional fluid global code [11] showed that an impurity radial flow inversion from inward to outward may occur in presence of a reversed shear due to a change of direction of the curvature pinch and to a modification of the dominant underlying instability.

Another recent theoretical achievement based on a gyrokinetic fluxtube code has shown that both rotation and shear rotation of the background plasma may play an important role especially for heavy impurities [5]: the E×B advection generates a pinch proportional to the background rotation with inward fluxes for TEM and outward fluxes for ITG modes. The Coriolis compression pinch leads instead to outward fluxes for TEM and inward fluxes for ITG. The effect increases with the charge number and with the mass to charge number ratio.

In [7] the centrifugal and Coriolis forces lead to significant outward advection especially for lower ionization states of massive impurities. The effect of plasma rotation on impurities was studied analytically in [32] to explain poloidal asymmetries in strongly rotating high collisionality plasmas.

Electromagnetic effects that may add to the electrostatic ones were studied in [Hein]. The contribution to impurity transport is mostly on the convective terms but remains typically quite small, of the order of 10% of the E×B term. Interestingly, also the direct effect on impurities of the electric fields associated with the injected RF power has been studied [30]. Apparently, the effect of the ponderomotive forces associated with the ICRF fields affect both the velocity and diffusion terms such that their ratio, the peaking factor of the impurity, is substantially preserved.

While impurities are in general considered in traces, so that the quasi-neutrality of the plasma is unaffected, a self-consistent treatment [10] has shown that, unlike the ITG case, in the case of TEM the contribution of impurities can be significant when their concentration is sufficiently high. The impact of the impurities on the instability pattern has also been matter of theoretical investigation in [25].

It is worthwhile recalling the results of the neoclassical theory on impurity transport which can be summarized in the simplified expression $v_{neo} / D_{neo} = Z_i \bullet (1/n \bullet dn/dr - H \bullet 1/T \bullet dT/dr)$ where n is the main fuel density, T is the main ion density assumed to be in equilibrium with the impurities and H is a factor close to 0.3. In the neoclassical framework therefore peaked density profiles attract impurities into the plasma centre while peaked ion temperature profiles have a screening effect.

In summary, a number of mechanisms have been studied to have a potential impact on the impurity transport while, on the other hand, there are only few examples of agreement between experiment and theory. In view of the use of W in ITER, the need to cast more light on the impurity behavior has motivated in JET a quantitative study of the effect of the addition of central electron heating on the transport parameter. The ICRH power scan applied in H minority has been performed in H-mode discharges dominated by Neutral Beam Power injection and with the injection of Ni and Mo in traces, via Laser Blow Off.

In the following we describe the experiment and its results and then discuss the role of turbulent instabilities and neoclassical effects in the determination of the impurity transport.

2. THE EXPERIMENT

The target plasma in which we have injected traces of Ni and Mo via LBO to study their transport behavior has been an H-mode discharge with 1.5MA of plasma current, 3 T of central toroidal magnetic field, relatively low triangularity = 0.15-0.3 (upper and lower respectively), q_{95} = 6-7 around 12MW of neutral beam power injected early enough in the discharge to keep the central safety factor q well above 1 to avoid sawteeth. It is well known that the latter are magnetic reconnection processes that expel impurities from the centre, with an effectiveness that depends on their frequency and the plasma volume involved. Their presence, however, inevitably adds complications in the impurity transport analysis and therefore has been avoided to discern the effect of central heating. The ICRH power has been injected in the plasma center and coupled to H minority , 5% concentration, in order to heat mainly electrons through collisions with the generated fast H ions. The start time of the ICRH power has been kept the same in all of the discharges. As a consequence, q has not been exactly conserved across the power scan resulting the higher the higher the extra power applied. Collisionality has been chosen to be low enough, $\nu_{eff} < 0.2$, to be ITER relevant (ν_{eff} = 10-14 $\langle n_e \rangle \langle T_e \rangle^{-2} Z_{eff} R$, with ne in m^{-3}, T_e in eV, R the major radius in m, the symbol $\langle\ \rangle$ denotes a volume average).

Table 1 contains the pulse database that has been built. The maximum RF power coupled to the plasma was 3MW. The neutral beam power has typically been 12MW, tough in a few discharges the tripping of one injector module has reduced the total NBI power by about 1.5MW. The radial profiles of the electron temperature, ion temperature, electron density, safety factor and plasma toroidal rotation at the time of the impurity injection are shown in Fig 1 for the discharges of the power scan with injection of Ni. The most apparent effect of the scan is on the profiles of ion temperature, toroidal rotation and safety factor. The density profile does not show any systematic change. Applying the Single Value Decomposition technique to the Thomson scattering and microwave interferometer data did not improve the quality of the density profiles.

To evaluate the transport properties of Ni and Mo, trace amounts have been injected via the LBO. If we assume that the impurity radial fluxes can be described as the sum of a diffusive and a convective contributions, $\Gamma_z = -D\, dn_z/d_r + vn_z$, the LBO injection is a perturbation of the impurity density that yields the convection v and the diffusion D transport parameters separately [20]. In stationary conditions and in absence of internal sources the so called pinch parameter $-v/D$ is just the normalized gradient of the impurity density.

For illustration purposes, Fig.2 shows for Pulse No: 74355 some time traces that characterize the LBO event and its impact on the discharge: a central bolometer channel, the line integrated electron density, the central ion temperature (from active charge exchange spectroscopy), the electron temperature from a central channel of the radiometer, Z_{eff} from Bremsstrahlung continuum, a central SXR chord and the brightness of the emission line from a relatively low ionization state such as Ni XVIII. The time of the injection of Ni was 5.3 sec. The impact of the injection of Ni is clear on bolometry soon after the laser pulse, when the Ni cloud crosses the relatively low temperature

edge, and modest on the line averaged density and Zeff. Ion and electron central temperatures are unaffected. A clear signal above the background appears on the SXR channel, which makes the analysis of the Ni transport feasible despite Ni is an intrinsic impurity in JET. The brightness of Ni XVII, as well as that of Ni XVIII emission lines, both from a survey spectrometer, has been used in the simulation codes as the time trace of the source term at the edge. The ionization potentials of Ni XVII and Ni XVIII are of 570 and 602 eV respectively and therefore these two states emit somewhere on the edge pedestal. This choice implies that the transport coefficient can be analyzed only in the region inside approximately $\rho = 0.7-0.8$.

To answer the legitimate question whether the LBO pulse itself is a cause of perturbation of the local plasma, so that the determined transport parameters may not be representative of the steady state regime, we observe that in the transport simulations reported below the resulting D's and v's do not need to be changed throughout the LBO pulse to allow a good reconstruction of the experimental radiation pattern, i.e. both during the fast period of penetration of the injected impurities into the plasma centre (around 10–50ms) and during the following longer phase of signal decay (200–300ms).

The analysis of nickel and molybdenum behavior during the LBO experiment has been performed by means of a one–dimensional (1D) collisional-radiative (CR) impurity transport model described in [22] that simulates available Ni /Mo spectroscopic lines, inverted SXR brightness and bolometer data. The procedure consists in varying in the impurity transport code the profiles of the diffusion coefficient and pinch velocity used as free parameters, until one obtains a satisfactory reproduction of the available radiation pattern in both the space and time domains. In order to perform an evaluation as objective as possible, such process is organized in terms of a χ^2 minimization procedure. Only those v's and D's profiles that lead to the reproduction of the Soft X-ray emission profile data within a chosen margin, typically 10%, are retained. The automatic routines have the advantage that they provide a range of uncertainty of the results, defined as the space filled by the class of D and v functions that are retained. In the following such range is used as an "error bar" in the plots showing the results, although it is important to state that they are not proper error bars. A proper error bar evaluation requires the knowledge of all of uncertainties of both the experimental data and the atomic data used in the analysis: such information is often hard to possess.

The nickel atomic data used in the model are those detailed in [23] while the atomic data for Mo are those referred to in [6]. The neoclassical drive of the Ni transport has been calculated by means of the code NCLASS [15]. In particular the NCLASS version coupled to the JETTO/SANCO transport code [17] has been used. Finally, to correlate the experimentally deduced transport parameters with the underlying turbulence the results of the H-mode discharges have been interpreted by the linear gyrokinetic code GS2 [16], where nickel in extremely low concentration fulfils the quasi neutrality condition when added to the two main species, deuterium ions and electrons.

3. RESULTS

The results of the transport analysis are summarized in Fig.3, showing the profiles of the transport parameters v and D used to simulate the LBO experiment with Ni and Mo injection in the discharges of Table 1. The effect of raising the ICRH power appears to affect primarily the convection parameter which starting from a relatively strong negative (inward) pinch in the reference case (Pulse No: 74354) with no RF power, moves towards less negative values and then reverses. Ni diffusivity instead features less important modifications, with perhaps a tendency to narrow the low transport region in the centre.

A summary of the results can be shown by plotting the -v/D ratio as a function of the applied RF power for two radial positions, $\rho = 0.2$ and 0.5 (see Fig.4). The results pertaining to Ni transport are represented by full circles (red online). Mo data are instead in full squares (blue online). Negative values of $-v/D$ mean that, extrapolated to stationary conditions, the impurity profile is hollow. For the radial position of $\rho = 0.2$ an amount of 1MW of ICRH already reduces the steepness of the Ni profile, which around 3MW become flat or reversed. The tendency found for Mo is similar. At $\rho = 0.5$1MW of ICRH seems to be sufficient to flatten the Ni profile. To visualize the effect of the power scan on the impurity profiles, the latter have been extrapolated to stationary conditions by means of the JETTO/SANCO code. Such code treats impurities in a predictive way, with the possibility to include neoclassical transport and, through a post processor, allows the simulation of the SXR lines of sight for an easy comparison with the experiment. The simulation has been run imposing the experimental transport parameters for long enough to reach the equilibrium. Examples of stationary Ni profiles are given in Fig.5 for three discharges of the power scan. In the reference discharge (Pulse No: 74354) the profile is well peaked starting from mid radius. As the power is applied the profile first becomes less peaked (Pulse No: 74356) and then hollow (Pulse No: 73460).

In plot 4, we have added other results of Ni and Mo transport analysis - open circles and squares symbols respectively - obtained in other discharges with similar but not identical ranges of toroidal field and plasma current, elongation , triangularity and collisionality but different ratios of ICRH to NBI power and/or different heating schemes as summarized in Table 2. In particular, in the two discharges with 4 and 5MW of ICRH, the RF power was injected according to the mode conversion scheme, with about 18% of He^3 used to swift the ion cyclotron frequency into the Bernstein waves domain, resulting in a much more localized electron heating profile peaked around $\rho = 0.1$. The discharge with 8 MW of coupled ICRH power was an L mode plasma, tough the input power was well above the L to H mode threshold. The added data seem to corroborate the picture that in the plasma centre the RF power induces a repulsion of the impurities more or less proportional to the injected power. At mid radius, in the so called confinement region, the extra heating is efficient to flatten the impurity profile for relatively low values of the RF power, but the change of the v/ D ratio is much smaller over the power scan. The latter finding is probably related to the fact that in this region diffusion is relatively large for all of the values of the RF power and in comparison the impact of convection is negligible.

3.1 DEPENDENCE OF THE RESULTS ON MAIN PLASMA PARAMETERS

The trend of the v/D ratio of impurities versus the applied RF power is quite a clear and robust result. However, the addition of central power on the same target discharge has a number of direct effects on several plasma parameters such that the identification of the mechanism that drives the change of the impurity flow is difficult. In fact, as seen in Fig.1, additional central heating modifies the q profiles, both the ion and electron temperature profiles and also the ion rotation profile. The effect on the electron density profile is less evident. Therefore the relationship between the impurity pinch parameter v/D and the ICRH power appears also in other parametric dependencies. In particular a very strong correlation exists between v/D of Ni and the normalized logarithmic gradients of the electron and ion temperatures, as shown in Figures 6 and 7 respectively. The higher the gradients the higher is the flattening effect on the Ni profile. Although not as strong, dependencies are found also with q, q shear and plasma rotation, as shown in Figures 8 and 9. The dependence on q and on q shear is weak. In particular outward flows would be connected with higher values of q and lower values of its shear. These dependencies should be studied in specific experiments with larger excursions of the parameters. Other dependencies, such as those on the density gradient or shear rotation are very poor and are not shown.

The discharges of the power scan have been carefully analyzed to check the presence of MHD modes, which could affect both heat and particle transport. The first three discharges with 0, 1 and 2MW of RF power respectively, do not show any significant sign of activity. Pulse No: 74359, with 3MW of ICRH, features an $m=3, n=2$ mode starting 1 second before the injection of Ni. The mode develops around $r/a=0.45$. Its amplitude is relatively small during the phase of the LBO pulse but is enough to leave a sizeable footprint in the electron temperature profile, like a small flattening. Only much later in the pulse, well beyond the Ni injection, a more important (2,1) mode is excited. Pulse No: 73460, with 3MW of ICRH power, is somewhat similar but the (3,2) mode persists only till 5.5 sec, that is in the middle of the LBO pulse that starts at 5.3s. The mode than evolves in a (4,3) mode before disappearing. In Pulse No: 73463, again 3MW of ICRH, there is no sign of relevant MDH modes. Summarizing, the macroscopic MHD instabilities do not interfere with the Ni transport experiments in the centre in all of the discharges. In two discharges with 3MW of ICRH there is some level of activity at mid radius. However, in a third discharge with same amount of RF power the Ni behaviour at mid radius is similar, so that it is reasonable to say that the identified MHD modes have no relevance in the determination of transport neither in the core nor at mid radius.

4. FLUXES DRIVEN BY ELECTROSTATIC INSTABILITIES

In order to identify the microinstabilities at work in the JET H-mode plasmas considered in this paper and evaluate their effect on the transport of Ni and Mo, the linear version of the gyrokinetic code GS2 has been applied. Simulations have included the analysis of the specific discharges of the RF power scan, where the main plasma parameters are those of the experiments, and also a parametric scan where, instead, starting from a situation close to the experimental one, one parameter at a time has

been modified over an interval to probe its specific role. In the simulations, impurities are included in a low (trace) concentration, $n_z/n_e = 5\ 10^{-5}$, in order not to perturb growth rate and frequency of the unstable modes, and to finally express the flux of the impurity species as a linear function of its logarithmic density/temperature gradients. In particular, for the quasi-linear impurity flux $\Gamma_z = \langle \delta n_z\ \delta v_{E\times B} \rangle$ the expression becomes $R\Gamma_z/n_z = D_z\ R/L_{nz} + DT_z\ R/L_{Tz} + Rv_{pz}$, with the coefficients D_z (diagonal diffusion), D_{Tz} (thermodiffusion) and v_{pz} (pure convection velocity) all independent of the logarithmic gradients. Alternately turning off/on the impurity gradients, the coefficients are easily computed. The pinch parameter can be finally rewritten as $Rv_z/D_z = C_P + C_T R/L_{Tz}$, with $C_P = Rv_{pz}/D_z$ and $C_T = D_{Tz}/D_z$ and L_{Tz} assumed to be equal to L_{Ti}. This procedure has been described extensively in [1, 2, 3].

Numerical calculations are electrostatic, collisionality is taken into account by means of a pitch angle scattering operator. Quasi neutrality conditions are satisfied. The coefficients C_P and C_T are computed for wavenumbers $k_y \sim 0.4$, i.e., corresponding to the maximum of the growth rate spectra.

For the experimental conditions of our H-mode plasmas, ITG modes are found to be largely dominant over the other instabilities. The results of this analysis are summarized in Fig 10 in terms of the pinch parameter $-v_z/D_z$ of Ni as a function of the RF power scan for the two radial positions at $\rho = 0.2$ and $\rho = 0.5$. As can be seen, if a slight decreasing trend exists between the simulated pinch parameter and the applied RF power, such decrement is far too small compared to the experimental value. The analysis of the effect of other plasma parameters, such as q , magnetic shear, R/L_{Te} or R/L_n on the Ni fluxes induced through the excitation of electrostatic instabilities shows that the general experimental trend is qualitatively reproduced with, however, a much lower rate. In Fig.7 the results of the simulations are compared to the experimental pinch parameters as a function of the normalized logarithmic gradient of the ion temperature.

In the simulations the pinch reversal is never reached despite the parameter scan is much larger than in the experiment, with the exception of the ion temperature gradient, which, for values lower than 2, much lower than in the experiment, causes an inversion of the mode rotation sign, in correspondence to a TEM-dominated turbulence. The Ni fluxes turn out to be mainly determined by the convection part, the thermodiffusion component being typically much smaller for high impurity charges such as Nickel.

5. THE NEOCLASSICAL CONTRIBUTION

In the previous chapter we have seen how the attempt to find a relationship between the experimental findings and the turbulence driven flows has shown that there may exist some analogies in the parametric dependencies, but in no way an outward flow can be expected on the basis of gyrokinetic simulations of these JET discharges. The other important and possible driver of radial impurity flows is the neoclassical term. In Fig.11 the neoclassical radial velocities computed by means of NCLASS for five of the discharges of the power scan are displayed. In all of the cases, in the regions of interest the neoclassical flow is relatively small and similar for all of the analyzed discharges, included

the reference one. There are no signs of trends as in the experiment either. To further investigate the influence of the found neoclassical terms on the overall behaviour of Ni a sensitivity study has been carried out by means of JETTO/SANCO runs, simulating the experiment with different choices for the velocity pinch. In Fig 12 we compare the simulations of the time evolution of the Soft X-Rays central channel, performed with different choices of the transport parameters: v and D from the experiment, v neoclassical and D from the experiment , v neoclassical and D such that v/D is identical to the experimental one, respectively. The simulation with the experimental v's and D's reproduces very well the experimental SXR time trace. In the other two cases the result is well outside any possible margin of error. We have also verified that the different time behavior of the various simulations, in particular the time required to reach the peak of the SXR emission after the impurity injection, is not due to differences in the transport parameters at the edge of the plasma.

6. DISCUSSION AND CONCLUSION

The scan of the ICRH power deposited in the plasma center of an H mode discharge with no sawteeth and with no or negligible MHD activity resulted in a sizeable change of the Ni and Mo transport. The transport parameters v and D of Ni and Mo have been measured by introducing small perturbations of the impurity densities via the laser blow off technique, which has the advantage of providing separately the values of convection and diffusion of the impurities. The analysis of the Soft X-Ray and spectroscopic data has been carried out by means of a 1-dimensional impurity transport code. In the power scan the pinch velocity v of the impurities is the term that experiences the most significant modification. The convection of Ni or Mo is inward in the reference case, with no extra power, reduces its amplitude as the RF power is applied and eventually changes sign, becoming outward directed, when the power exceeds approximately 3MW. The effect is pronounced in the plasma centre, around $\rho = 0.2$, while in the middle of the minor radius the flattening effect does occur but mitigated by the relatively large diffusion. In terms of Ni or Mo profiles in the plasma core extrapolated to the stationary case, the changes induced by the RF power are from a peaked profile to flat and then hollow. The result of the scan confirms a more general trend observed in a less homogeneous set of JET discharges, as it is shown in Fig.4. Ni and Mo seem to be affected in a similar way.

The additional ICRH power does not affect only the impurity profiles. The injected power increases both the ion and temperature gradients in the centre, raises the safety factor in the centre, affecting also its profile, and the plasma rotation increases. It is therefore impossible to associate the change in the impurity velocity uniquely to a particular plasma parameter. The correlation between the pinch parameter and $-R/L_{Ti}$ between 6 and 9 is however remarkably good. Such strong a correlation is lost for instance in the relationship with the plasma rotation. Pulse No: 74360, which had one neutral beam injector box less and therefore less momentum input, is clearly outside the trend indicated by the other discharges in Fig.10. The correlation between the Ni pinch parameter and the electron temperature is also quite good. The one with q, its shear and the rotation shear are

instead relatively poor. The linear dependence of the pinch parameter on $-R/L_{Ti}$ clearly recalls that of the neoclassical theory where v_{neo}/D_{neo} is proportional to the difference between the logarithmic gradients of density and temperature. In these discharges the electron density profile does not change significantly and -R/Lne is always below 3, that is relatively small, which would emphasize the role of the thermal screening. The agreement between neoclassical theory and experiments is however only qualitative: the absolute value of the neoclassical convection computed for the discharges of the power scan is up to an order of magnitude smaller than in the experiment, as seen in Fig.11. In addition we have shown how the estimated neoclassical velocities do not allow a good reconstruction of the experimental time traces of the SXR signals.

We have also evaluated in Chapter 5 the impurity pinch driven by the electrostatic turbulence. The impurity fluxes computed in GS2 simulations for the most unstable modes, show that in the parameter space spanned by the experiment the conditions for an impurity flow inversion are never reached. A flow inversion in order to occur would require an R/L_{Ti} lower than 2 while keeping all of the other parameters unchanged. This confirms results obtained in [34] for other JET H-mode discharges. It is also interesting to note that one of the main difference between the present JET discharges and those of ASDEX Upgrade where the impurity outflow was successfully simulated by turbulent codes [2] is that JET features indeed higher ion temperature gradients and lower electron temperature gradients.

In conclusion, the scan of centrally deposited ICRH power in JET low collisionality H-mode discharges has confirmed that a few MW can avoid the formation of peaked Ni and Mo profiles. In a practical sense this result is important in view of the use of W in JET and ITER. The exact mechanism providing this effect is not yet clear although the strong correlation of the Ni pinch parameter with the logarithmic ion temperature gradient suggests that the flattening effect is of neoclassical origin. The fact that the absolute values of the neoclassical convection velocities do not fit with the experimental ones constitutes a discrepancy that is to be clarified.

ACKNOWLEDGMENT

A thankful thought goes to Mario Mattioli. This work was supported by EURATOM and carried out within the framework of the European Fusion Development Agreement. The views and opinions expressed herein do not necessarily reflect those of the European Commission.

REFERENCES

[1]. C. Angioni and A.G. Peeters, Physical Review Letters **96**, 095003 (2006)

[2]. C. Angioni, R. Dux, E Fable, A G Peeters et al . Plasma Physics and Controlled Fusion **49** 2027 (2007)

[3]. C. Angioni, A.G. Peeters , G.V. Pereverzev et al., Nuclear Fusion **49** 055013 (2009)

[4]. R. Burhenn, Y. Feng K Ida et al Nuclear Fusion **49** 065005 (2009)

[5]. Y. Camenen, A.G. Peeters, C. Angioni et al., Physics of Plasmas **16**, 012503 (2009)

[6]. L. Carraro, L. Gabellieri, M. Mattioli et al Plasma Physics and Controlled Fusion **46** (2004) 389–407
[7]. K.G. McClements and R.J. McKay Plasma Physics and Controlled Fusion **51** 115009 (2009)
[8]. R. Dux, R. Neu, A.G. Peeters, et al. Plasma Physics and Controlled Fusion **45**, 1815 (2003).
[9]. Estrada-Mila, J. Candy, R.E. Waltz Physics of Plasmas **12** 022305 (2005)
[10]. T. Fulop and H Nordman Physics of Plasmas **16** 032306 (2009)
[11]. S. Futatani, X. Garbet, S. Benkadda, N. Dubuit, PRL **104**, 015003 (2010)
[12]. C. Giroud, C. Angioni, G. Bonheure, et al., "Progress in understanding impurity transport at JET," FEC 2006, Chengdu, Paper No. EX/8-3, (2006).
[13]. P. Gohil, L.R. Baylor, K.H. Burrell et al., Plasma Physics and Controlled Fusion **45**, 601 (2003).
[14]. R. Guirlet, D. Villegas, T. Parisot et al Nuclear Fusion **49** 055007 (2009)
[15]. W.A. Houlberg, K.C. Shaing, S.P. Hirshman, M.C. Zarnstorff, Physics of Plasmas **4** (1997) 3230
[16]. M. Kotschenreuther, G. Rewoldt, and W.M. Tang, Comput. Phys.Commun. **88**, 128 (1995).
[13]. L. Lauro- Taroni, B. Alper, R. Giannella et al et al . Proc. Eur. Conf on Contr. Fusion and Plasma Physics, Montpellier, France, ECA, 18B, 102 (1994),
[18]. ITER Physics Expert Groups on Confinement and Transport and Confinement Modeling and Database, Nuclear Fusion **39**, 2175 (1999).
[19]. M. Leigheb M Romanelli L Gabellieri et al. Plasma Physics and Controlled Fusion **49** 1897 (2007)
[20]. E.S. Marmar, J.L. Cecchi and S.A. Cohen Review of Scientific Instruments **46**, 1149 (1975)
[21]. E.S. Marmar, B Bai, RL Boivin et al., Nuclear Fusion **43**, 1610 (2003). Fusion **45**, 2011 (2003).
[22]. M. Mattioli, K B Fournier, I Coffey, et al., Journal of Physics B **34**, 127 (2001).
[23]. M. Mattioli, K B Fournier, L Carraro et al., Journal of Physics B **37**, 13 (2004).
[24]. S. Menmuir, L Carraro, A Fassina et al., Plasma Phys. Control. Fusion 52 095001(2010)
[25]. S. Moradi, M. Z. Tokar, and B. Weyssow, Physics of Plasmas **17**, 012101 (2010)
[26]. V. Naulin JJ Rasmussen C Angioni et al AIP Conf. Proc. 1013, 191 (2008). Turbulent Transport in Fusion Plasmas: First ITER International Summer School Conference Proceedings
[27]. M.F.F. Nave, J Rapp, T. Bolzonella et al., Nuclear Fusion **43**, 1204 (2003).
[28]. R. Neu, R. Dux, A. Geier et al. , Plasma Physics and Controlled Fusion **44**, 811 (2002).
[29]. R. Neu, R. Dux, A. Kallembach et al, Nuclear Fusion, **45**, 209 (2005)
[30]. H. Nordman R. Singh T. Fulop et al Physics of Plasmas **15** 042316 (2008)
[31]. J.E. Rice, P.T. Bonoli, E.S. Marmar et al., Nuclear Fusion **42**, 510 (2002).
[32]. M. Romanelli, M Ottaviani., Plasma Physics and Controlled Fusion **40**, 1767(1998).
[33]. M.E. Puiatti et al., Plasma Physics and Controlled Fusion **44** 1863 (2002)
[34]. M.E. Puiatti, M Valisa, C. Angioni et al., Physics of Plasmas **13** 042501 (2006)

[35]. M.E. Puiatti, M Valisa, M. Mattioli et al., Plasma Physics and Controlled Fusion
[36]. H. Takenaga, S Higashijima, N. Hayashi et al., Nuclear Fusion **43,** 1235 (2003).
[37]. E. Scavino, J Bakos, H Weisen et al., Plasma Physics and Controlled Fusion **46**, 857 (2004)
[38]. Villegas et al. PRL 105, 035002 (2010)
[39]. M.R. Wade, W.A. Houlberg, and L.R. Baylor , Physical Review Letters **84** 282 (2002).

Discharge	Ip (MA)	B(T)	NBI (MW)	ICRH(MW)	Minority species	LBO
74354	1.5	3	12	0	H	Ni
74355	1.5	3	12	1	H	Ni
74359	1.5	3	12	3	H	Ni
74360	1.5	3	10.7	2.9	H	Ni
74363	1.5	3	10.5	2.9	H	Ni
74357	1.5	3	12.5	0	H	Mo
74362	1.5	3	10.5	3	H	Mo

Table 1: Discharge database, indicating plasma current, toroidal field, injected power via NBI and IRCH, minority species for ICRH heating and the species injected via LBO.

Shot	Ip MA)	Bt (T)	NBI(MW)	ICRH(MW)	Minority species	LBO
58143	1.8	3.27	13.6	4.7	He3	Ni
58149	1.8	3.27	14.6	5.1	He3	Ni
66432	1.8	3.35	20	2	He3	Ni
66434	1.8	3.35	20	2	He3	Ni
68383	2.3	3.2	8.3	8	H	Ni
69808	1.8	3.2	11	0	H	Ni
68381	2.3	3.2	9	8.45	H	Mo

Table 2: Other JET discharges featuring Ni or Mo Laser Blow Off injection used for general considerations of the effect of ICRH power on impurity profiles.

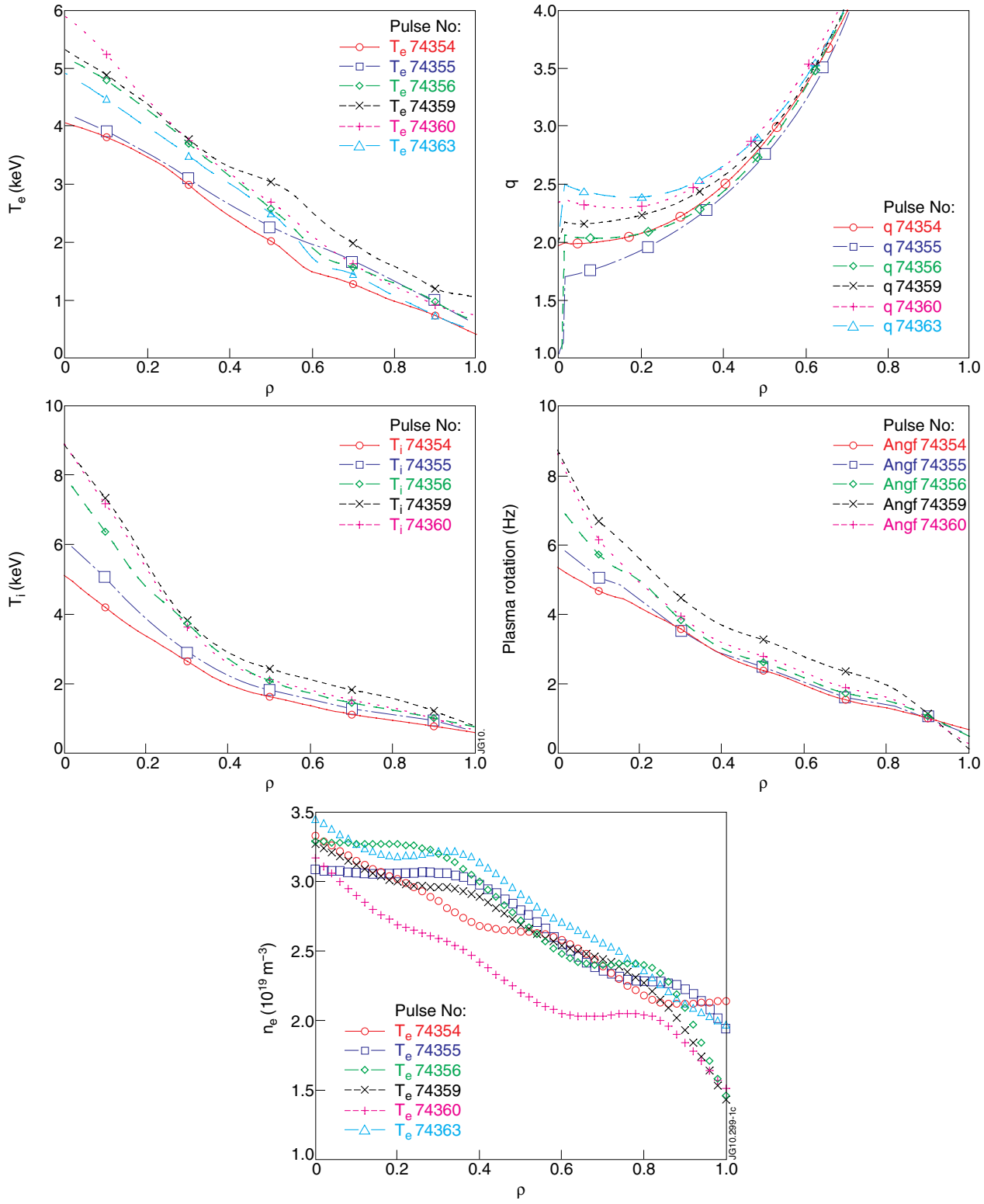

Figure 1: For the discharges of the power scan at the time of the Ni injection; on the right from top to bottom: Radial profiles of electron and ion temperature electron density. On the left: safety factor and plasma rotation.

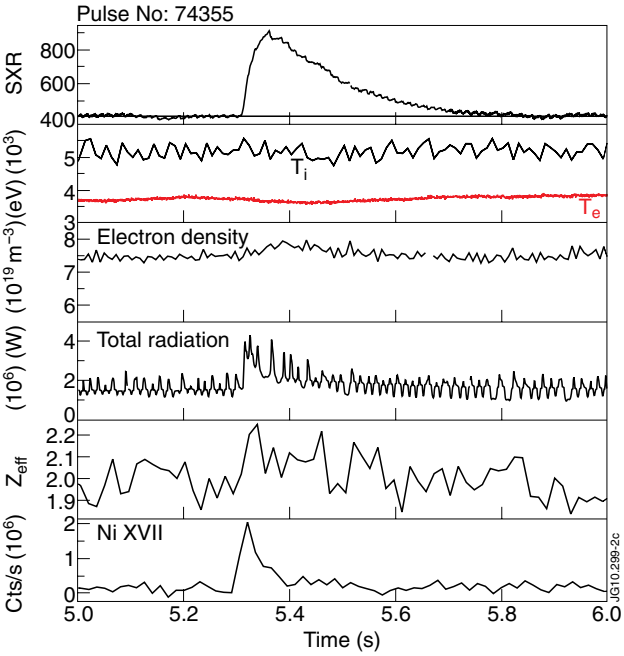

Figure 2: Effect of the injection of Ni on (from top) one central SXR chord, T_e(squares) and T_i, line integrated n_e, bolometer and emission of $Ni17^{+.}$

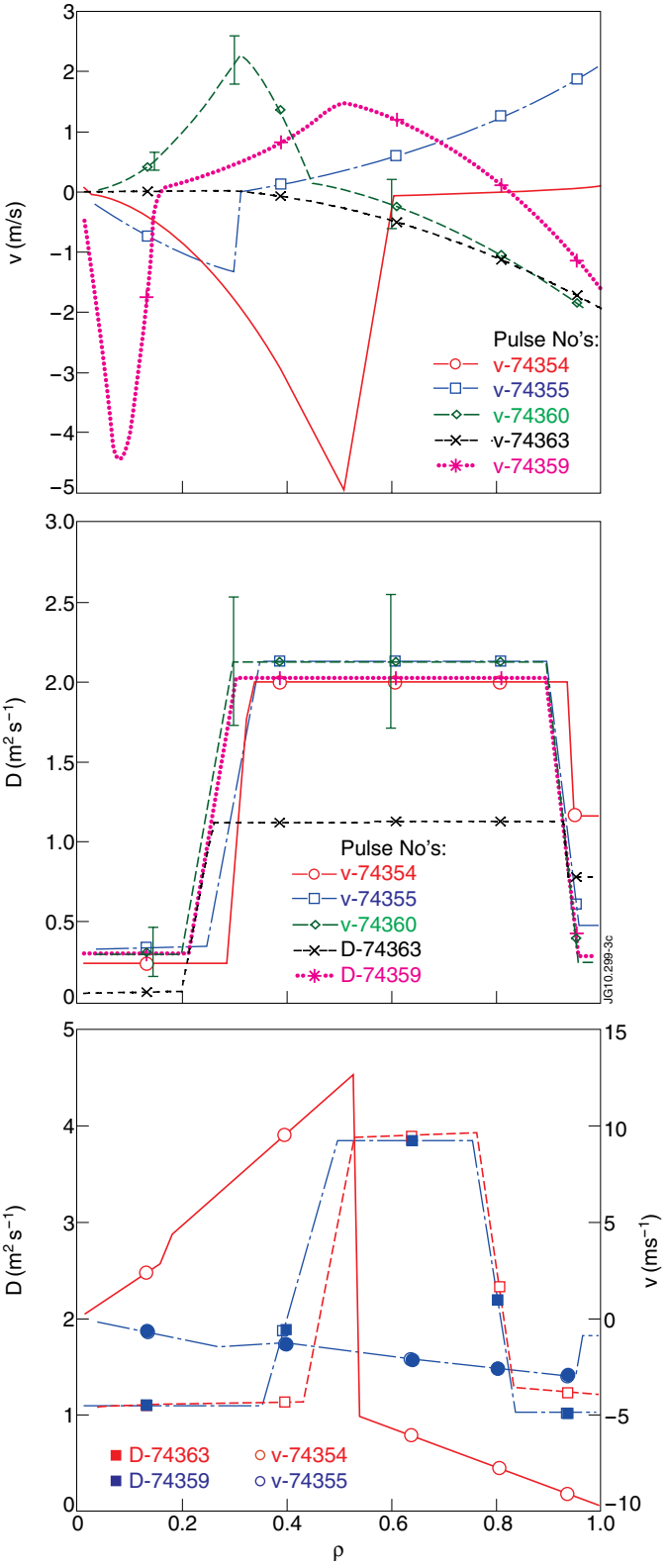

Figure 3: Radial profiles of the transport parameters v (top) and D (middle) used to obtain the best simulations of the nickel injection in the discharges of the power scan. Those indicated for Pulse No: 74360 are not error bars but the region of the parameter space where simulation replicate the experimental evidence within +/- 10%. The bottom plot shows v and D for the two discharges with Mo injection.

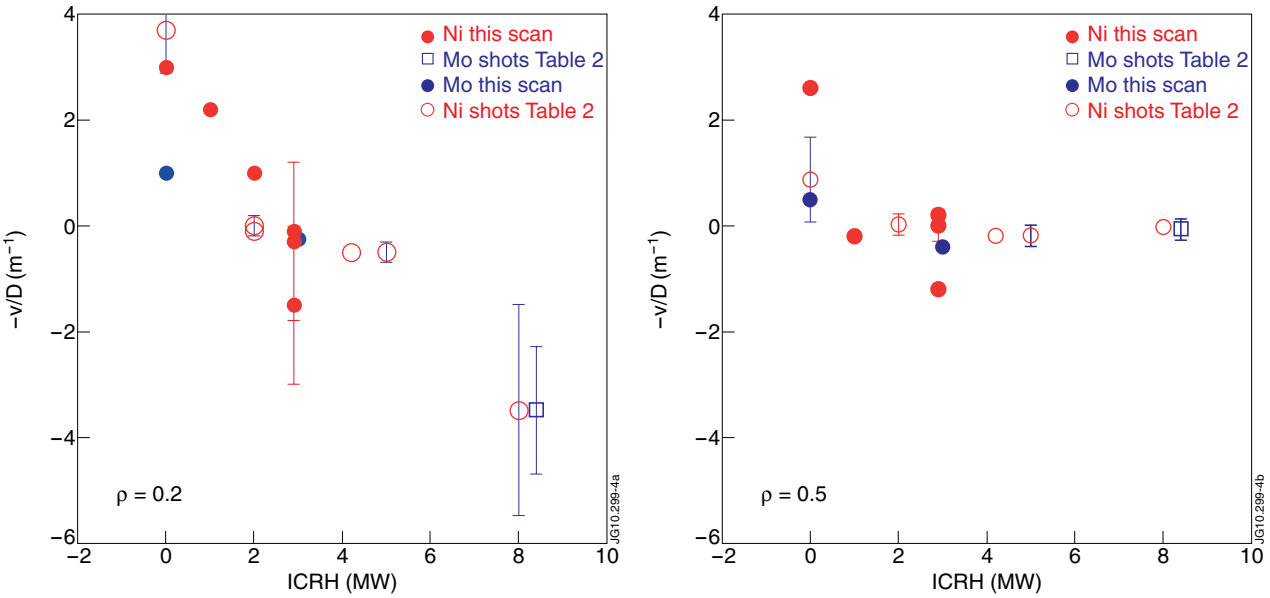

Figure 4: Pinch parameter at (top) ρ = 0.2 and (bottom) ρ = 0.5 of: Ni (full circles, red online) and Mo (full squares, blue online)in the discharges of the power scan; Ni (open circles) and Mo (open squares) in the JET discharges listed in Table 2.

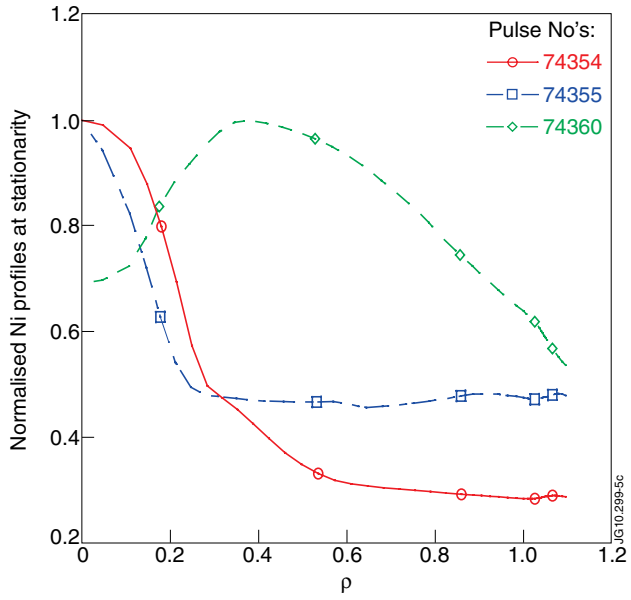

Figure 5: Ni density profile extrapolated to stationary state for three discharges with no power (Pulse No: 74354), 1MW (74355) and 3MW (74360) of ICRH respectively. Profiles are normalized at their maximum. 1MW of RF power reduces the central peaking and 3MW make the profile hollow.

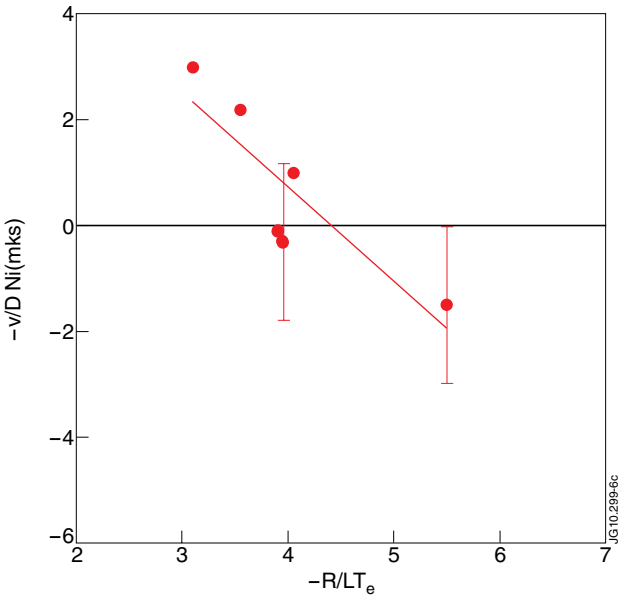

Figure 6: Relationship between the pinch parameter -v/D of Ni and the logarithmic electron temperature gradient for the shots of the power scan listed in Table 1. A linear fit to the data is also drawn.

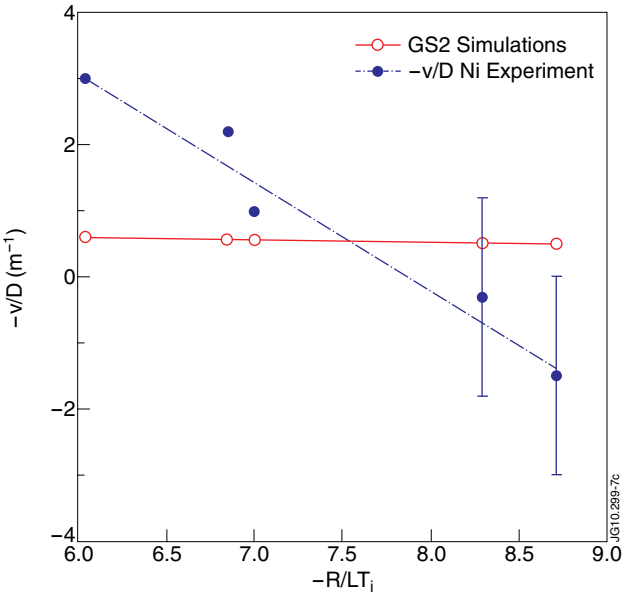

Figure 7: Relationship between the pinch parameter –v/D of Ni and the logarithmic electron temperature gradient for the shots of the power scan listed in Table 1. The experimental results (full symbols) are compared with the quasi linear simulations (open circles). A linear fit to the data is also drawn.

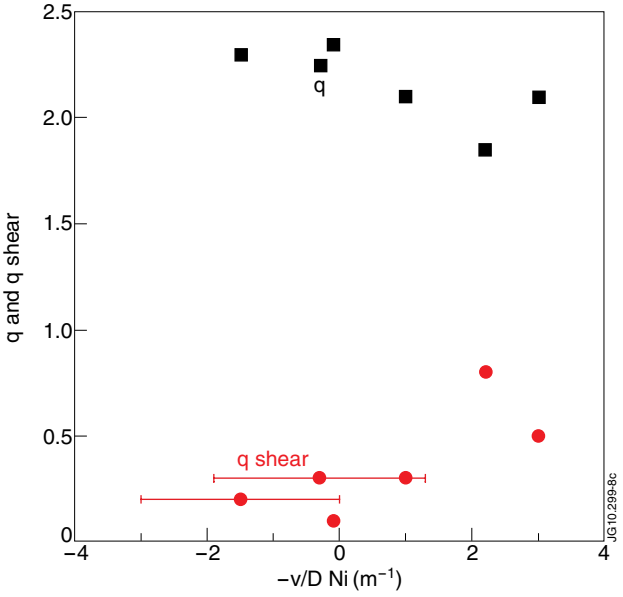

Figure 8: Dependence of the pinch parameter –v/D of Ni on q and 1/q dq/dρ for the shots of the power scan listed in Table 1.

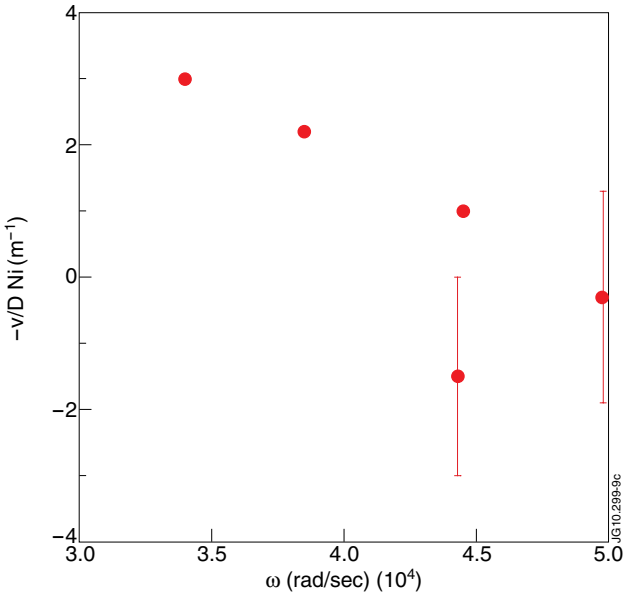

Figure 9: Dependence of the pinch parameter –v/D of Ni on the toroidal rotation ω for the shots of the power scan, listed in Table1, with the exception of Pulse No: 73463where rotation data were missing.

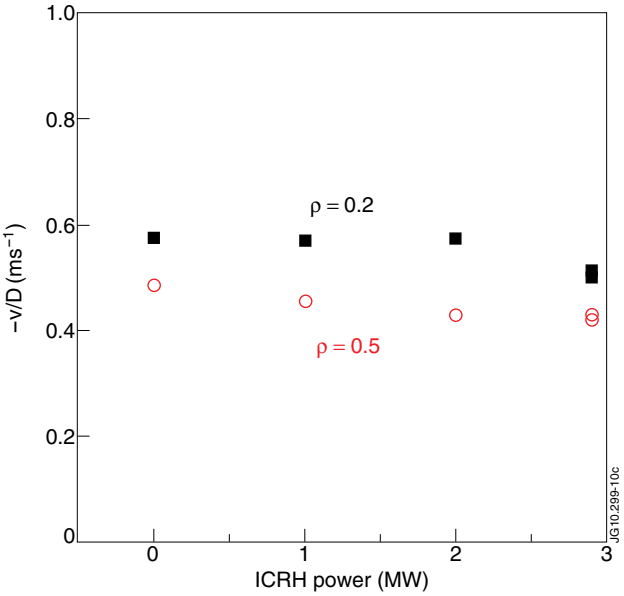

Figure 10: The pinch parameter –v/D of Ni predicted by GS2 for the discharges of the ICRH power scan at ρ = 0.2 and ρ = 0.5 . The variation is much smaller than in the experiment and, especially, there is no flow inversion.

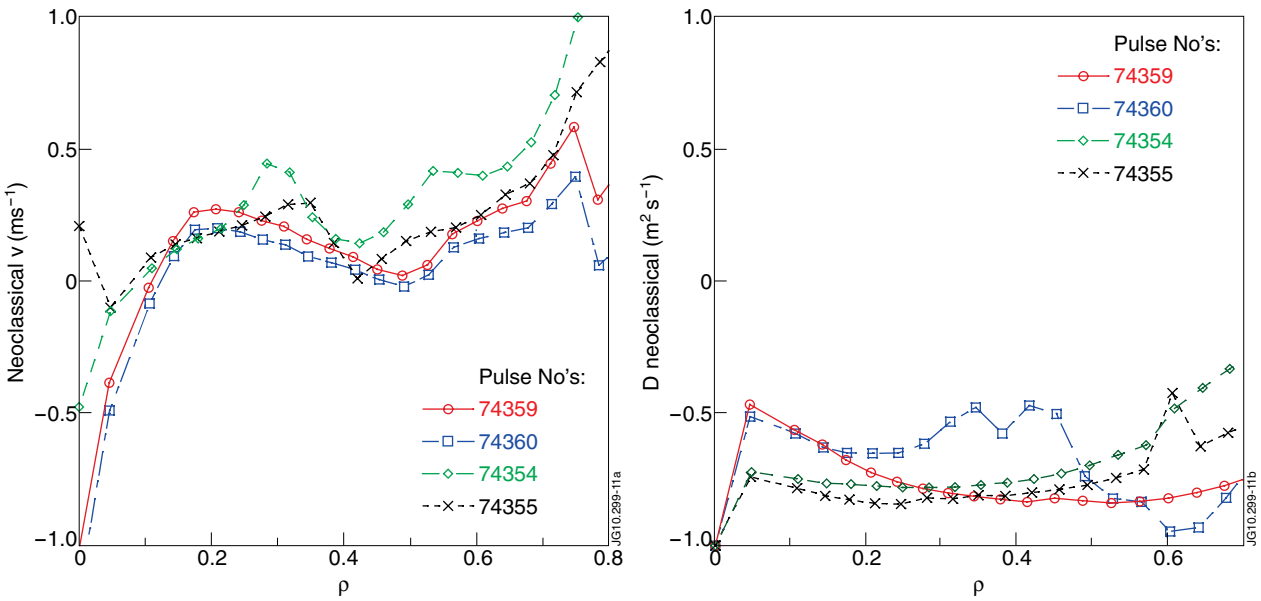

Figure 11: Radial profiles of neoclassical v (top) and D (bottom) for the discharges of the power scan at the time of the Ni injection.

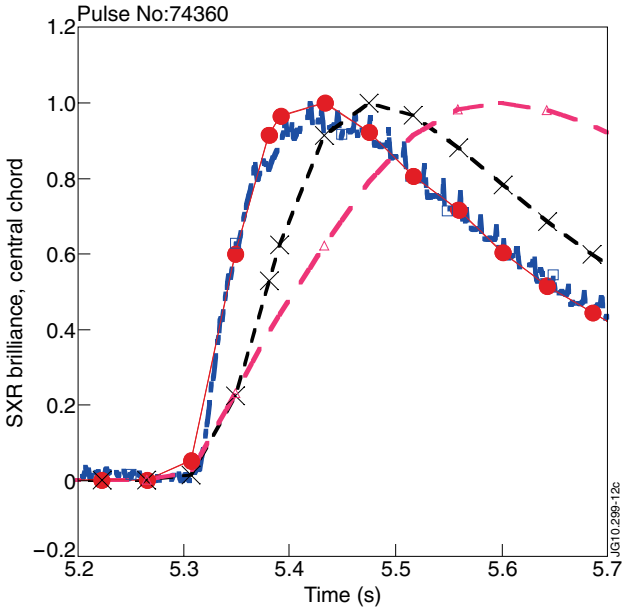

Figure 12: Simulation of the chord integrated central SXR emission (normalized) during the injection of Ni in Pulse No: 74360. Continuos line: experiment. Full circles: simulation with transport parameter from experiment. Short dashes: simulation with v neoclassical and D from experiment. Long dashes: v